Telecommunication Systems (2023) 82:363–379
https://doi.org/10.1007/s11235-023-00990-x

Textile monopole sensors for breast cancer detection

Dalia M. Elsheakh[1,3] · Soha A. Alsherif[2] · Angie R. Eldamak[2]

Accepted: 31 December 2022 / Published online: 21 January 2023

Abstract
This paper presents two flexible monopole antennas implemented on cotton substrate as sensors designed for radar-based microwave imaging and particularly breast imaging systems. The flexible antennas are basic building block of a radar-based microwave imaging system that could be integrated in clothes. Thus, these low-cost textile sensors could be used by women for self-monitoring and early breast cancer detection at an affordable price. The ultra-wideband fully textile sensors are designed as rectangular and circular monopole antennas. Both sensors have an impedance bandwidth ≤ -10 dB from 2.2 to 8 GHz with an overall footprint of 50×50 mm^2. Simulations for antenna in proximity to breast model with and without tumor as well as bending capacity are performed. The simulations are complemented with fabrication of a breast phantom and a tumor sample with parameters that mimic these of the human breast's healthy and malignant tissue. Measurements are compared to simulation results as well as the performance of antenna before and after subjected to washing. Finally, the specific absorption rate is also calculated and measured to ensure safety for on-body deployment. The proposed work demonstrates the potential to develop wearable microwave imaging system using fully textile antennas.

Keywords Breast cancer · Flexible antenna · Textile sensor · Cancer detection · Wearable technologies

Abbreviations

MI	Imaging techniques
UWB	Ultra-wideband
SAR	Specific absorption rate
BCD	Breast cancer detection
WHO	World health organization
MRI	Magnetic resonance imaging
PET	Positron emission tomography
CT	Computed tomography
LAR	Lifetime attributable risk (LAR)
DAK	Dielectric assessment kit
NM	Not mention
SIW	Substrate integrated waveguide
GCPW	Ground coplanar waveguide

✉ Dalia M. Elsheakh
dalia-mohamed@buc.edu.eg; daliaelseakh@eri.sci.eg

Soha A. Alsherif
Soha.alsherief@gmail.com

Angie R. Eldamak
angie.eldamak@eng.asu.edu.eg

[1] Department of Electrical Engineering, Faculty of Engineering and Technology, Badr University in Cairo, Cairo, Egypt

[2] Electronics and Electrical Communications Engineering Department, Faculty of Engineering, Ain Shams University, Cairo, Egypt

[3] Microstrip Department, Electronics Research Institute, El Nozha, Cairo, Egypt

1 Introduction

Breast cancer is expected to have around 11% percent death rate in 2020, according to WHO Cancer Country profiles. This puts Breast cancer as the second leading cause of cancer-related death in Egypt after liver cancer [1–5]. According to an analysis of breast cancer in 187 countries, the occurrence of breast cancer has drastically increased from an average of 641,000 cases in 1980 to an average of 1,643,000 cases in 2010. Cancer is an asymptomatic disease in the early case, in which the patient experiences no evident symptoms or pain until the cancer progresses to an advanced stage [1]. These unsettling statistics demonstrate how early detection and diagnosis of cancer can be crucial for improving survival rates. Regular and safe screening can be used to keep track of this. Women over the age of 40 should get at least a scan once a year as a good role of thumb. Mostly for young

women, breast cancer is diagnosed at a later stage and at higher grade with greater chance of recurrence [5]. Thus, early cancer detection is critical for successful medical treatment and cure [2]. There are plenty of methods are being used for cancer screening such as: Mammography, breast ultrasound, thermography, magnetic resonance imaging (MRI), positron emission tomography (PET), optical imaging, electrical impedance based imaging, and computed tomography (CT) [6, 7]. Mammography is a widely used imaging technique for detecting breast cancer. It is a combination of ultrasound and x-ray imaging, where the malignant tissue appears brighter. It helped decreasing the mortality rate in screened women by 25% to 30%. Despite its undeniable success, mammograms fail in detecting cancer in its early stages and in denser breasts. It's also an expensive technique that a large portion of the population may find it difficult to access regularly [7].

CT scans are another form of X-ray imaging. Because they usually have low contrast, iodine injections are required to create a brighter, clearer picture. However, CTs are not suitable for routine scans, despite being mildly invasive [1]. Ultrasound imaging uses sound waves to form real-time images. On its own, it causes unacceptable false positive and false negative outcomes in asymptomatic women. MRIs, on the other hand, are beneficial to women who are at a higher risk of breast cancer and can be used to assess dense breasts. Its downside is that it's unable to detect early-stage cancer, takes a long time to perform, not readily available in all places, and is costly [2]. As more evidence accumulated, it became clear that non-traditional imaging methods for breast cancer imaging were required. One that is non-ionizing, cheaper and more accessible. Although Microwave imaging techniques (MWI) is relatively recent, it showed competence to fill this uprising need. The benefits of MWI include the fact that it is non-ionizing, non-expansive, and non-invasive. Microwave-based breast cancer imaging systems are promising low-cost sensing tools due to the high contrast between normal tissue and tumors. It also balances the competing requirements for resolution and penetration depth with high potential to detect small tumor at short scanning time [1, 2]. It can reduce safety hazards due to its non-ionizing nature, allowing women to receive regular breast cancer screening compared to other existing techniques [2]. The basic idea behind microwave imaging is to use one or more antennas to illuminate the target object, and then use receive antennas to capture the scattered field surrounding the target domain. The scatter data is then processed to reconstruct a map of the imaging domain.

Scattering data processing in MWI relies on the electrical characteristics of normal and malignant breast tissues [10]. Microwave Imaging (MWI) restores the scanned image using the reflected wave from the internal breast with tumor [6, 7]. It observes changes in reflection or transmission and compares the dielectric characteristics of normal and malignant breast tissues [6]. Several research studies support using MWI as an alternative to mammography in early diagnosis for breast cancer [6–11]. In these systems, the antenna is positioned in proximity with the human body as a single element or in arrays [2, 12]. As a result, antenna development and optimization are critical in determining the overall performance of a detection system. In addition to the newly used flexible and textile antennas, other antenna types have been described in the above-mentioned imaging systems [1, 6, 7, 11–19].

Wearables have proven to be a valuable technology for imaging systems due to its low cost, low profile, thinness, and robustness, as well as its potential to be integrated into human clothing [13, 14]. Development of wearable antennas has increased due to increasing demand for continuous health monitoring applications, rapid connectivity, and IoT deceptions. The developed wearable antennas are mostly planar, specifically microstrip patch antennas, because they mainly radiate perpendicularly to the planar structure and their ground plane efficiently shields the human body [15]. Several factors affect the performance of the flexible antenna/ sensor. This includes chosen substrate, the fabrication technique as well as frequency range [16]. Three types of substrates have often surfaced in the fabrication of flexible antennas: thin glass, metal foils, and plastics or polymer substrates [16]. Many conductors are suited and have previously been used in the manufacture of flexible antennas. Silver conductor yarn, Metal-nano particles (silver and copper), conductive polymers, graphene-based materials and liquid metals [2].

Few numbers of research groups are working on developing wearable microwave imaging systems for breast cancer detection or imaging with textile sensors [6, 7, 9, 13–19]. The wearable system from Montreal University reported in [6, 7, 9] uses flexible microstrip antennas to easily develop to a wearable system, and flexible substrate for the PCB that provides all signal routing, system assembly and calibration. The wearable flexible system consists of 16 monopole antennas arranged in an array that operates between 2 and 5 GHz and is embedded in a bra [7, 9]. The antennas will be in contact with the skin by placing it on the inner surface of the bra. This placement excludes any uncertainty regarding the breast position relative to the measuring system and sensors. In [9], monopole antennas are fabricated on Kapton flexible substrate to maintain adequate coverage of the breast and allows elements to take the shape of the breast.

In [13], a compact UWB purely textile monopole antenna is developed that is applicable to be embedded in wearable microwave imaging systems. Polyester fabrics serve as the substrate, with conductive copper polyester taffeta fabric serving as the radiating elements and ground. The antenna structure in [13] shows two triangles and a few parallel slots to increase the current path. This results in an UWB range from

1.198 to 4.055 GHz (109%). In [13], measurements in contact with tissue-mimicking phantoms with little effect on the operation of the antenna are conducted. In [14], an embroidery triangular textile antenna with shorting pins is proposed at 5.8 GHz with bandwidth 210 MHz. Under bending conditions, the antenna in [14] maintains safe SAR values and stability. Though the antenna in [14] acquires 4.1 dBi gain, it acquires only 3.8% bandwidth which does not fit imaging applications. Moreover, the effect of washing cycles on the antenna performance was not addressed. Textile substrates are increasingly being used for wearable antennas and sensors since they provide comfort and flexibility at a low cost [13]. Thus, the designed textile antennas combine traditional textile materials with new technologies and acts as interface of the human-technology-environment [13].

In [17], an UWB antenna designed on a denim substrate, a Shield It conductive textile with thickness of 0.17 mm and fed through a substrate integrated waveguide (SIW) transition and ground coplanar waveguide (GCPW) with an overall size of 60 × 50 × 0.7 mm is proposed. It realizes broadband impedance BW of 7–28 GHz and maximum gain of 10.5 dBi. The antenna's performance in free space and in proximity to breast to detect a tumor in different considerations is tested. Reconstructed images in [17] proved that the antenna can part of a wearable WBAN system for breast cancer monitoring and imaging. In [18], another wideband, low profile, fully flexible, and all-textile-based slotted triangular antenna loaded with a 2 × 2 textile-inspired artificial magnetic conductor to be worn on the wrist is proposed. Though the proposed antenna in [18] realizes low SAR levels of 3.28 × 10^{-6} and 9.37 × 10^{-7} W/kg at 3.5 and 5.8 GHz, it covers a frequency band from 3.1 to 6.5 GHz and maximum realized gain of 7.82 dBi with a footprint of 36 × 18 × 3 mm.

In this paper, a fully textile UWB monopole antennas with size 50 × 50 × 2 mm are presented and proposed in several shapes as shown in Fig. 1. The proposed antennas are designed with the potential of integration into women's clothes for monitoring breast and detecting any abnormalities in its tissues. Reflection $|S_{11}|$ and Transmission $|S_{21}|$ coefficients are collected and compared for the proposed sensor with and without tumor inserted in a breast phantom model. This paper is extension to the work published in [19] which included rectangular shaped monopole only. The study in [19] only include simulations of rectangular monopole in proximity to breast phantom with and without tumor as well as measurements in air (wet & dry). In [19], The flexible antenna uses cotton as substrate with low dielectric loss, relatively low permittivity, low coefficient of thermal expansion, and high thermal conductivity where a conductive thread or fabric had been used. However, in this paper, breast and tumor phantom models are synthesized, fabricated and characterized. Measurements in proximity to breast phantoms with and without tumor are also added and presented. Moreover, a comparative study of shape of radiator either rectangular or circular in terms of sensing over body is included as well as comparison with similar structures in literature. The proposed antenna offers easier fabrication routine compared to textile-based antennas presented in [17, 18] with comparable performance.

The organization of the paper after an introduction is as follows: Section II presents design and simulation of proposed textile antennas in both rectangle and circular shapes for radiators. Section III demonstrates the measurements of the proposed textile antennas. Section IV shows the simulations of proposed antennas including breast phantom models. Section V presents the measurements of proposed textile antenna in proximity to breast phantom model. Finally, conclusions show in section VI.

2 Methods/experimental

In this paper, textile technology is chosen to build all proposed structures. This implies that radiator, ground and substrate are composed of textile materials. Regarding the substrate, Cotton is favoured among other textile alternatives [18]. This owes to its good properties in terms of comfortable, absorbing human sweat, no allergy, easy fabrication, low price as referred to in [9, 15, 19]-[20–25]. Data of several textile materials that can be used as substrate is reported in [18] as well as fabrication challenges. Among these, effects of washing cycles on fabric, developing a precise pattern, controlling accuracy of dimensions as well as some fabrics are not suitable enough to develop wearable antenna [20, 25]. Cotton substrate has rated electrical properties: dielectric constant (ε_r) of 1.4–1.8 and loss tangent (tan δ) of 0.05–0.08 with height of 2 mm [21–23]. Two proposed textile monopole antennas are studied and compared in FCC band from 2.2 to 8 GHz with dimensions width (W_s) of 50 mm and length (L_s) of 50 mm for the substrate.

The first monopole acquires a radiator with rectangular shaped with width (W) of 17 mm, length (L) of 22 mm. While the ground plane has width (W_s) of 50 mm, and length (L_g) of 17 mm. On the other hand, the second monopole antenna with circular shape has radius (R) of 14 mm, feeding length (L_f) of 16 mm. Ground plane for circular-shaped monopole has width (W_s) of 50 mm, and length (L_g) of 14.7 mm. A 50 Ω transmission feeding line (W_g) of 3 mm is shown in Fig. 1a for rectangular patch while 3.2 mm for circular one as shown in Fig. 1b. Two types of conductors were assigned in simulations for radiators and ground plane. The first one is copper clad conductor with thickness 0.5 mm while the second one is sliver conducting fabric with sheet resistance of 0.5 Ω/square. The given dimensions and simulations are chosen after optimization through two different electromagnetic field simulators; CST studio suite

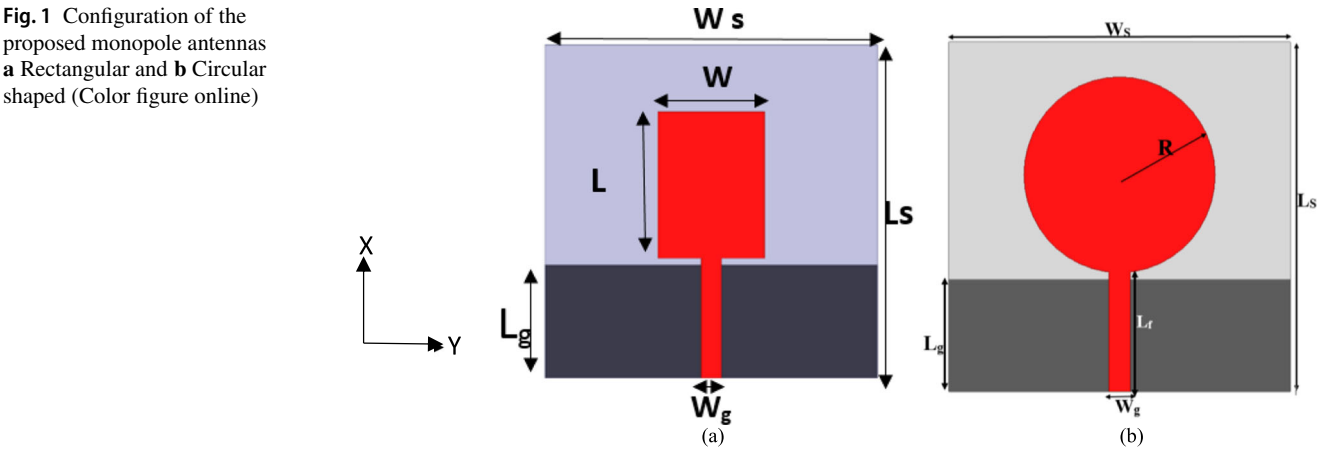

Fig. 1 Configuration of the proposed monopole antennas **a** Rectangular and **b** Circular shaped (Color figure online)

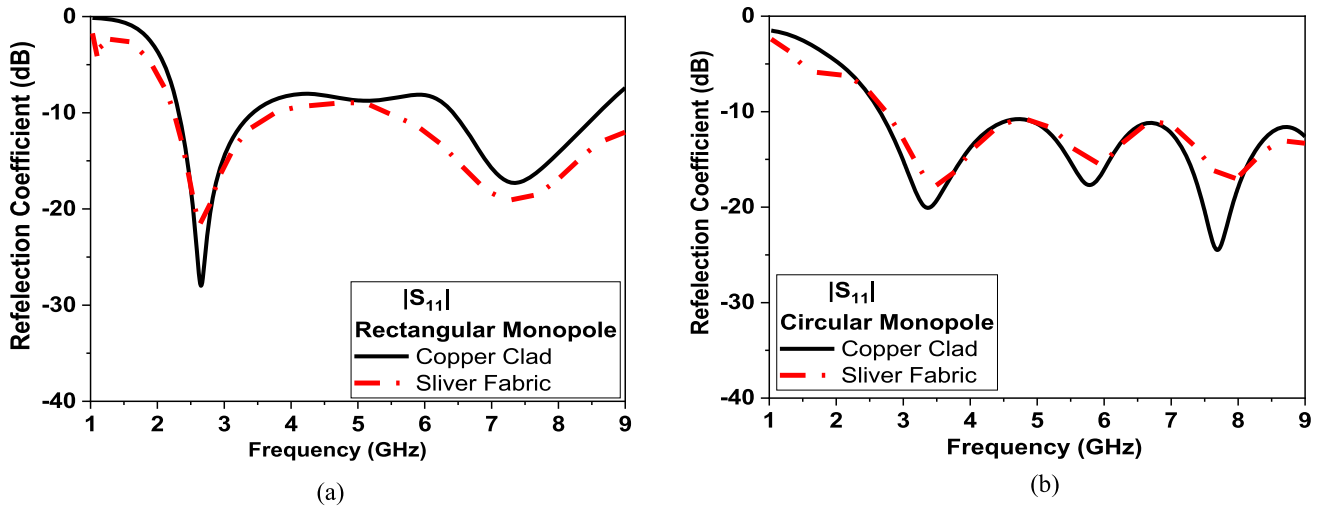

Fig. 2 Simulated reflection coefficient in dB for the two antennas using copper clad and Sliver conducting fabric for monopole antenna **a** rectangular and **b** circular (Color figure online)

Ver. 2020 and high frequency structure simulation (HFSS) ver. 17. From the reflection coefficient results, comparable performance is recorded with both types of conductors for rectangular and circular monopole antennas at Fig. 2a, b, respectively.

Moreover, the gain of the proposed shaped antennas using both conductors are simulated and compared in Fig. 3a, b. Figure 3 shows that the simulated gain for both proposed monopole antennas using copper clad conductor is higher than textile fabric for frequencies less than 3 GHz. While in the frequency range from 3 to 5 GHz rectangular monopole antenna acquire similar gain values, while the other antenna shape has 4 dBi gain difference. Thus, textile conductors could be used in building radiators and ground for the proposed antennas.

3 Measurement results

The two proposed antennas are fabricated as shown in Fig. 4a and Fig. 5a. Both figures show the front and back view of the antennas. Both antennas are tested and measured using a vector network analyzer (Anritsu MS4647A). The magnitude of reflection coefficient ($|S_{11}|$ in dB) for both measured and simulated data for both antennas are shown in Figs. 4b, 5b. The rectangular monopole antenna has measured reflection coefficient of − 29 dB, − 40 dB at 2.5 GHz and 6.3 GHz while − 20 dB, − 18 dB at 3.1 GHz and 5.5 GHz for circular monopole antenna. As the proposed antennas are anticipated to be embedded in clothes as on-body sensors, the effect of wetting conditions is also included in the study. This is realized by recording the response of the fabricated antennas at dry, immersing the antenna in tape-water container (wet condition) and after getting dry. The wet response for both proposed prototypes (rectangular and circular) are shown in Fig. 6a, b.

From measurements, both antennas preserve its response after immersing in water and dry out. Thus, they could be embedded in clothes to act as on-body sensors to monitor vital signs or for cancer screening. Though the proposed structures act as wearable sensors, the far field radiation properties are

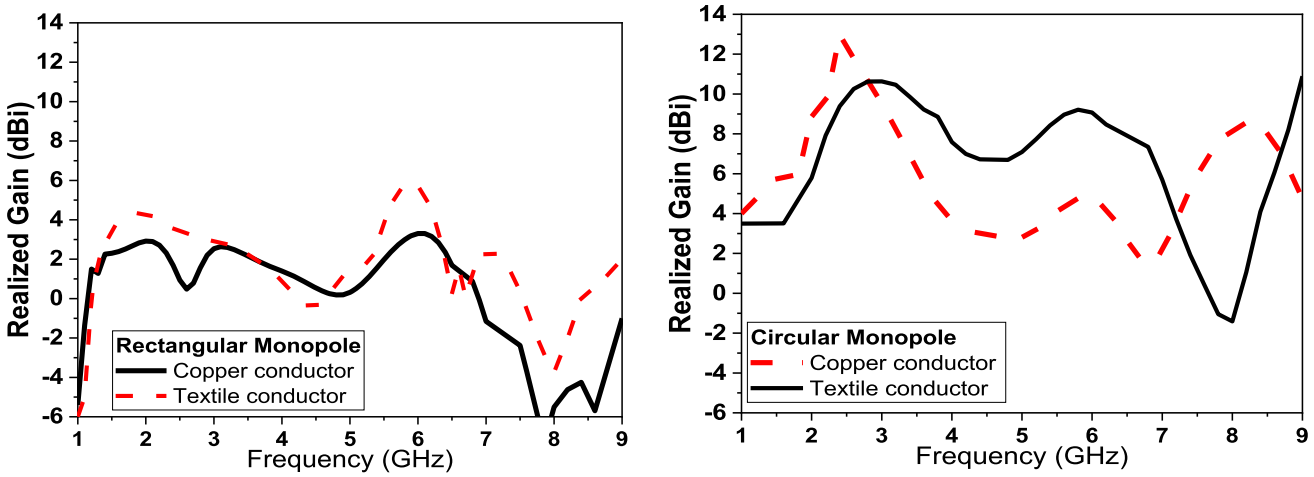

Fig. 3 Simulated gain versus frequency for the two antennas using copper clad and Sliver conductive fabric for monopole antenna **a** rectangular and **b** circular (Color figure online)

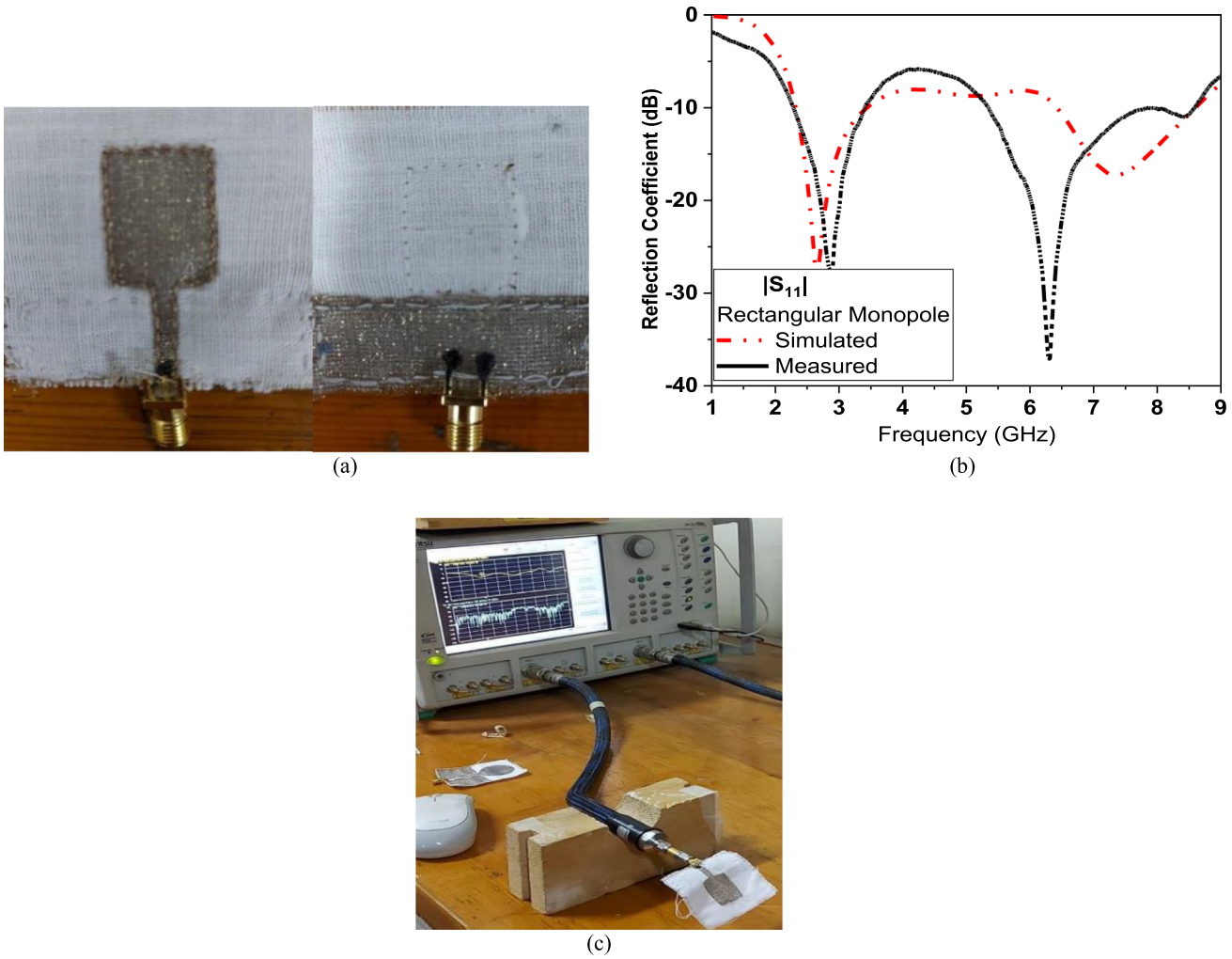

Fig. 4 **a** Fabricated rectangular monopole antenna showing front & back views, **b** Reflection coefficient (($|S_{11}|$ in dB) of the prototype (Simulated and Measured) and **c** photo of setup measurements of rectangular monopole antenna (Color figure online)

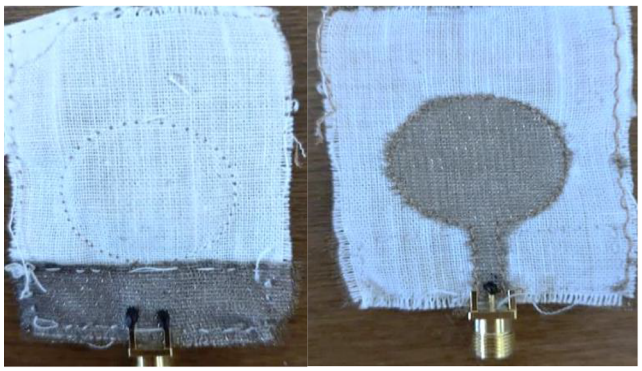

(a)

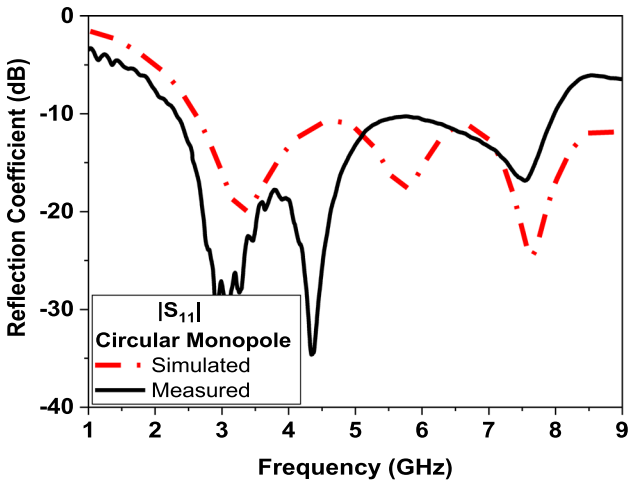

(b)

(c)

Fig. 5 **a** Fabricated circular monopole antenna showing front & back views, **b** Reflection coefficient (($|S_{11}|$ in dB) of the prototype (Simulated and Measured) and **c** photo of setup measurements of circular monopole antenna (Color figure online)

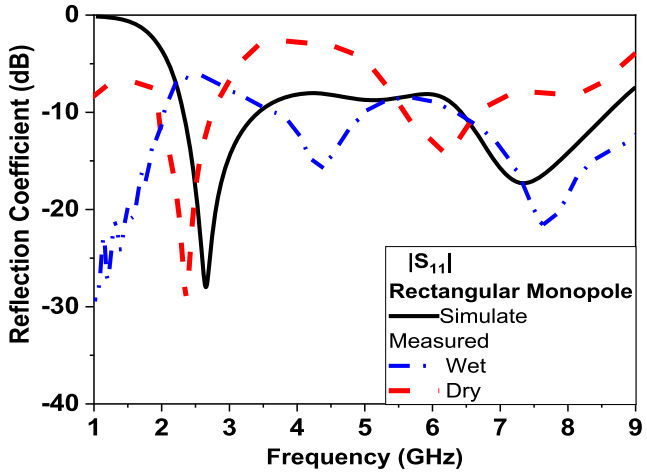

(a)

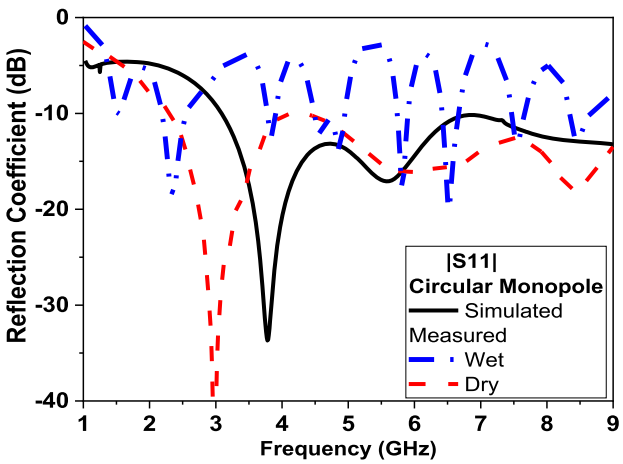

(b)

Fig.6 Antenna reflection coefficient at wet and dry condition **a** rectangular monopole and **b** circular monopole (Color figure online)

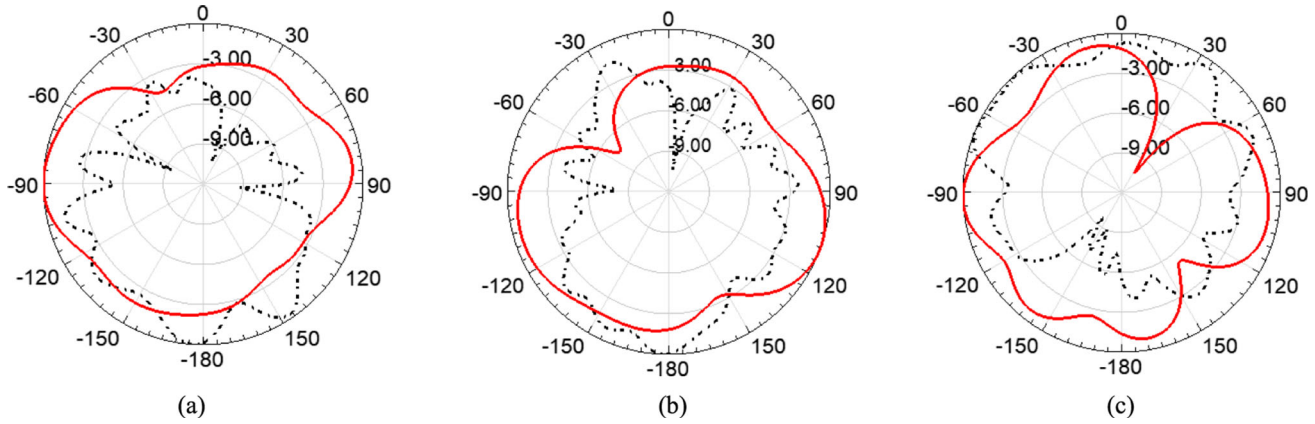

Fig. 7 The 2D polar radiation pattern of rectangular monopole antenna **a** $\Phi = 0°$, **b** $\Phi = 90°$, and **c** $\theta = 90°$ at 2.5 GHz, proposed antenna in free space (solid red) and on body (dash black) (Color figure online)

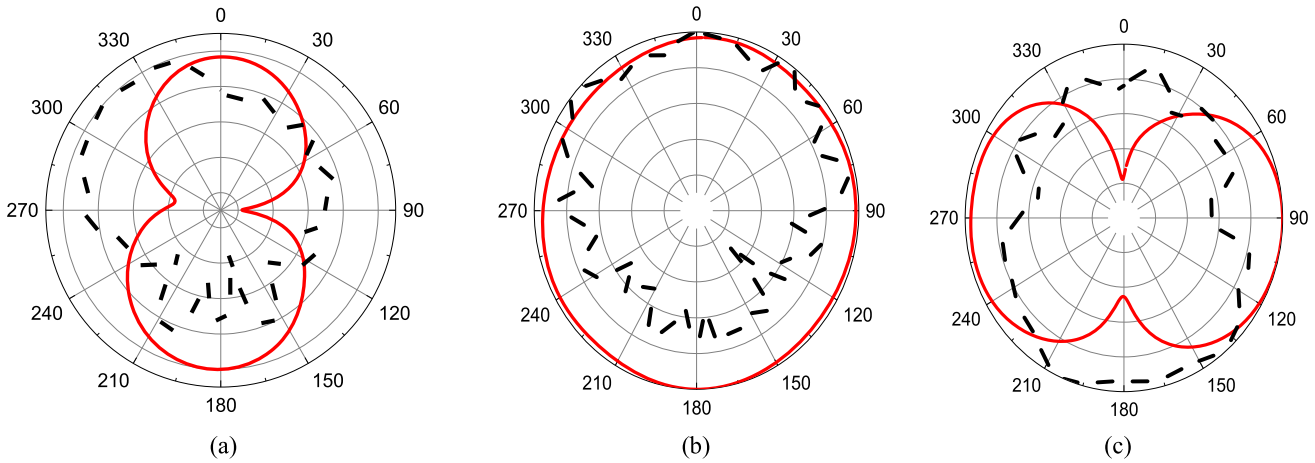

Fig. 8 The 2D polar radiation pattern of circular monopole antenna **a** $\Phi = 0°$, **b** $\Phi = 90°$, and **c** $\theta = 90°$ at 2.5 GHz, proposed antenna in free space (solid red) and on body (dash black) (Color figure online)

recorded in Fig. 6 and Fig. 7 at phi = 0°, 90° and theta = 90°. The radiation patterns for proposed monopole antennas with rectangular and circular are recorded in both free space and when mounted on body are shown in Fig. 7a–c and Fig. 8a–c at resonant frequencies 2.5 GHz and 3.1 GHz. Though, there are many repels created when the antennas are placed on body, omnidirectional operation are still maintained.

Given that textile antennas are flexible and conformal, the effect of bending antennas in both X- and Y- directions are simulated and recorded. Different bending angles of 0°, 45°, 75° and 90° are used in simulations and presented in Figs. 9, 10. From given figures, it could be concluded that rectangular shaped antennas maintain its operation after subjected to bending in either X- or Y-directions compared to circular one.

4 Simulations of textile antenna in proximity to breast phantom model

The basic composition of a human breast is glandular tissue, adipose tissues (fat), fibrous tissues covered with a skin layer [23]. A survey for the most suitable phantoms for imitating human breast is listed in [23–27]. Breast are classified into four classes according to their density where: mostly fatty, scattering fibro glandular, heterogeneously dense and, extremely dense [24, 25]. Breast density will affect the dielectric properties as it simply represents the amount of fat or fibro glandular tissues. The ideal microwave breast phantom should mimic the electromagnetic properties of the heterogeneous breast tissues, its geometry, provide an easy way to insert the tumor phantom and it should be durable for long periods. Three major classes are found for such phantoms as chemical phantoms (oil in gelatin mixtures can mimic the four types of breasts by varying the percentage of oil in the

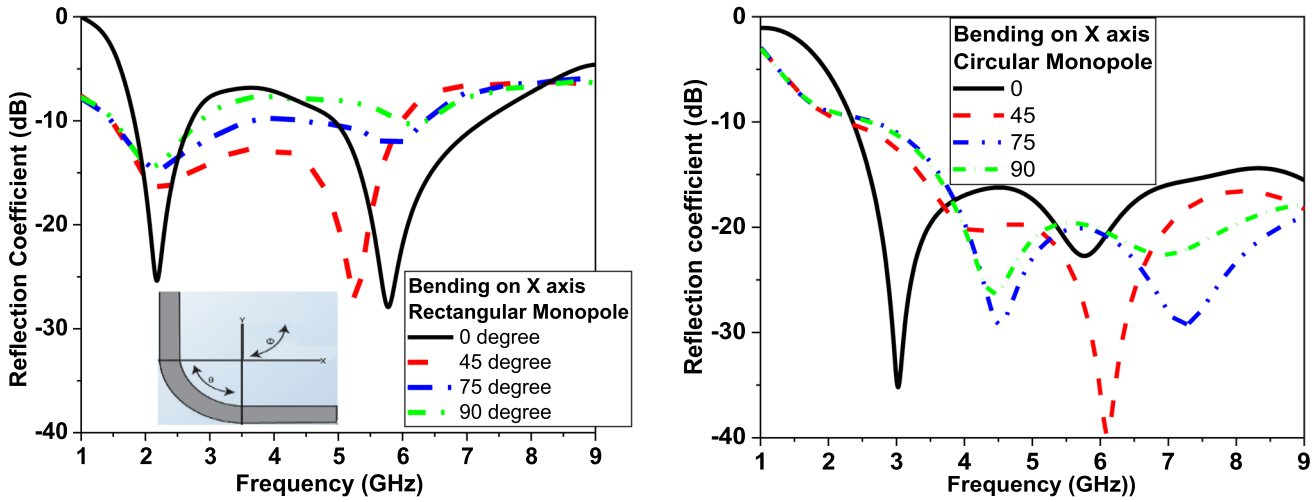

Fig. 9 The effect of bending on X axes monopole antennas performance **a** Rectangular shaped and **b** Circular shaped (Color figure online)

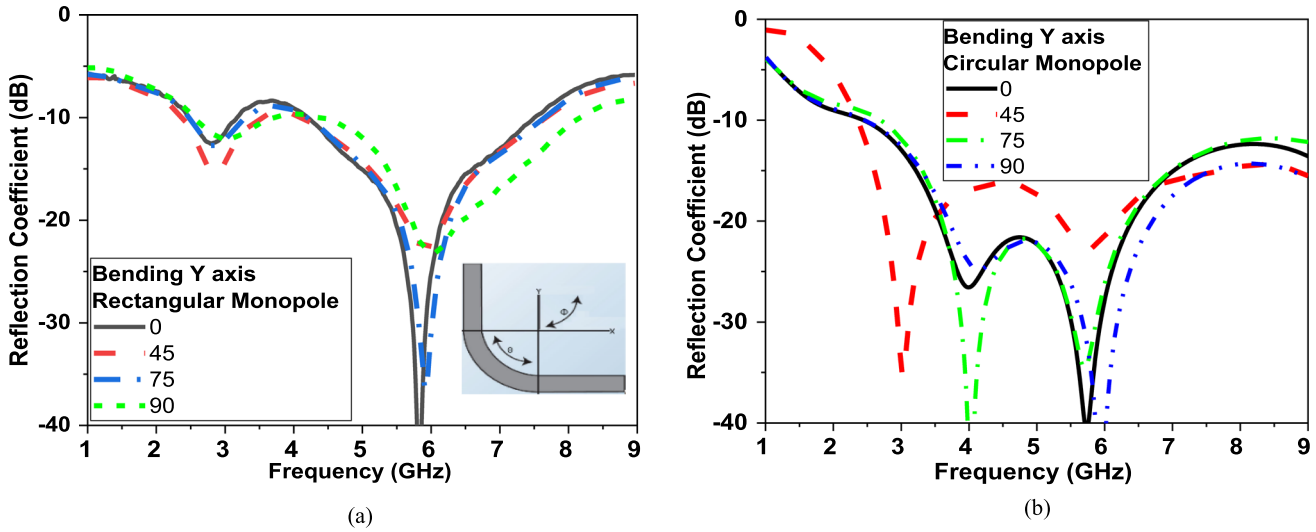

Fig.10 The effect of bending on Y axes monopole antennas performance **a** Rectangular shaped and **b** Circular shaped (Color figure online)

mixtures), numeric phantoms (provided by different simulation programs prove to be the most accurate in mimicking breast tissues, as CST) and 3D printed phantoms.

The performance of the two proposed antennas (rectangular & circular monopoles) in contact to breast tissues with and without tumor will be studied. The dimensions and electrical properties of the four-layer phantom model embedded in simulation are presented in [19, 26] and shown in Fig. 11. The tumor size used in the simulation is 10 mm diameter with electrical properties as reported in [9] and shown in Fig. 11. The tumor is placed at distance 60 mm approximately in the center of the phantom. In the given study, two simulation scenarios were adopted. The first scenario starts by placing one sensor/ antenna in contact to breast phantom as shown in Fig. 11a while the second scenario using two sensors/ antennas at two opposite sides of the breast model as shown in Fig. 11b. These two scenarios will allow recording the reflection coefficient (S_{11}) and transmission coefficient (S_{21}). In all simulations, the antenna is positioned above the breast with 2 mm filled with cotton substrate as illustrated in Fig. 11b. Results shown in Figs. 12–15 are the simulations using breast tissue models with and without tumors [8, 27].

Figures 12, 13 show magnitude and phase of reflection coefficient for both rectangular and circular monopoles with and without tumor, respectively. Figure 12 shows that the tumor increased the magnitude of the reflection coefficient by 1 dB and induced a shift of 100 MHz at lower resonant band at 1.1 GHz for rectangular monopole. At higher resonant frequency at 5 GHz, it changes the magnitude of reflection

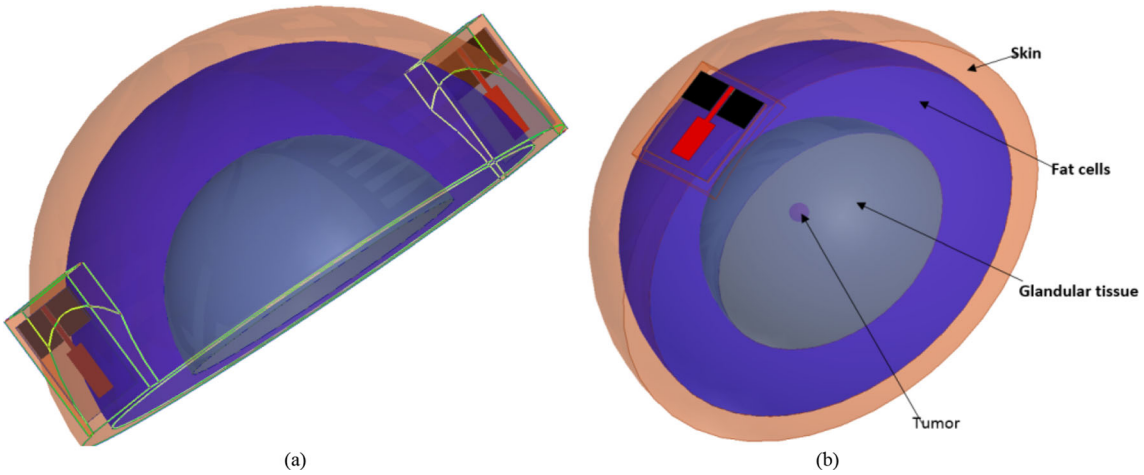

Fig.11 Three layers model of breast in [15] with and without tumor tested using **a** one antenna and **b** two antennas (Color figure online)

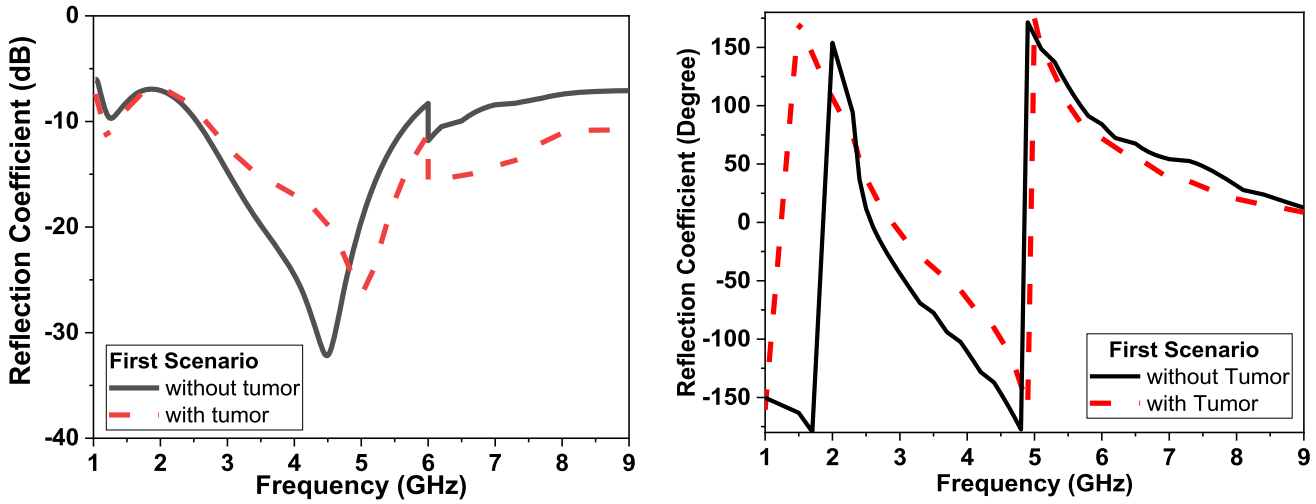

Fig.12 Simulated |S11| of rectangular monopole antenna with and without tumour $|S_{11}|$ **a** magnitude in dB and **b** phase in degrees (Color figure online)

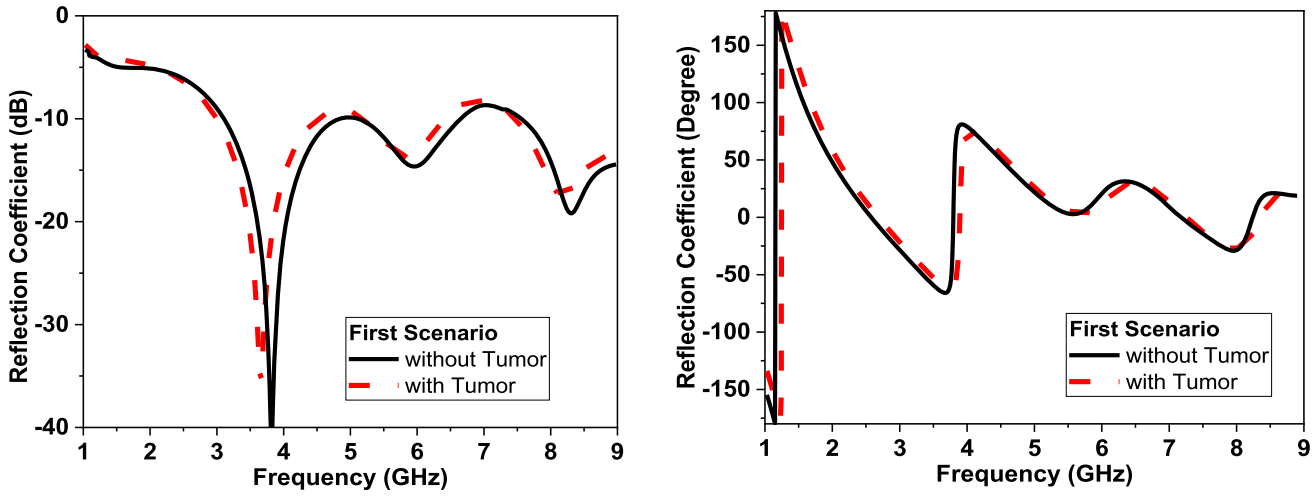

Fig.13 Simulated |S11| of circular monopole antenna with and without tumour $|S_{11}|$ **a** magnitude in dB and **b** phase in degrees (Color figure online)

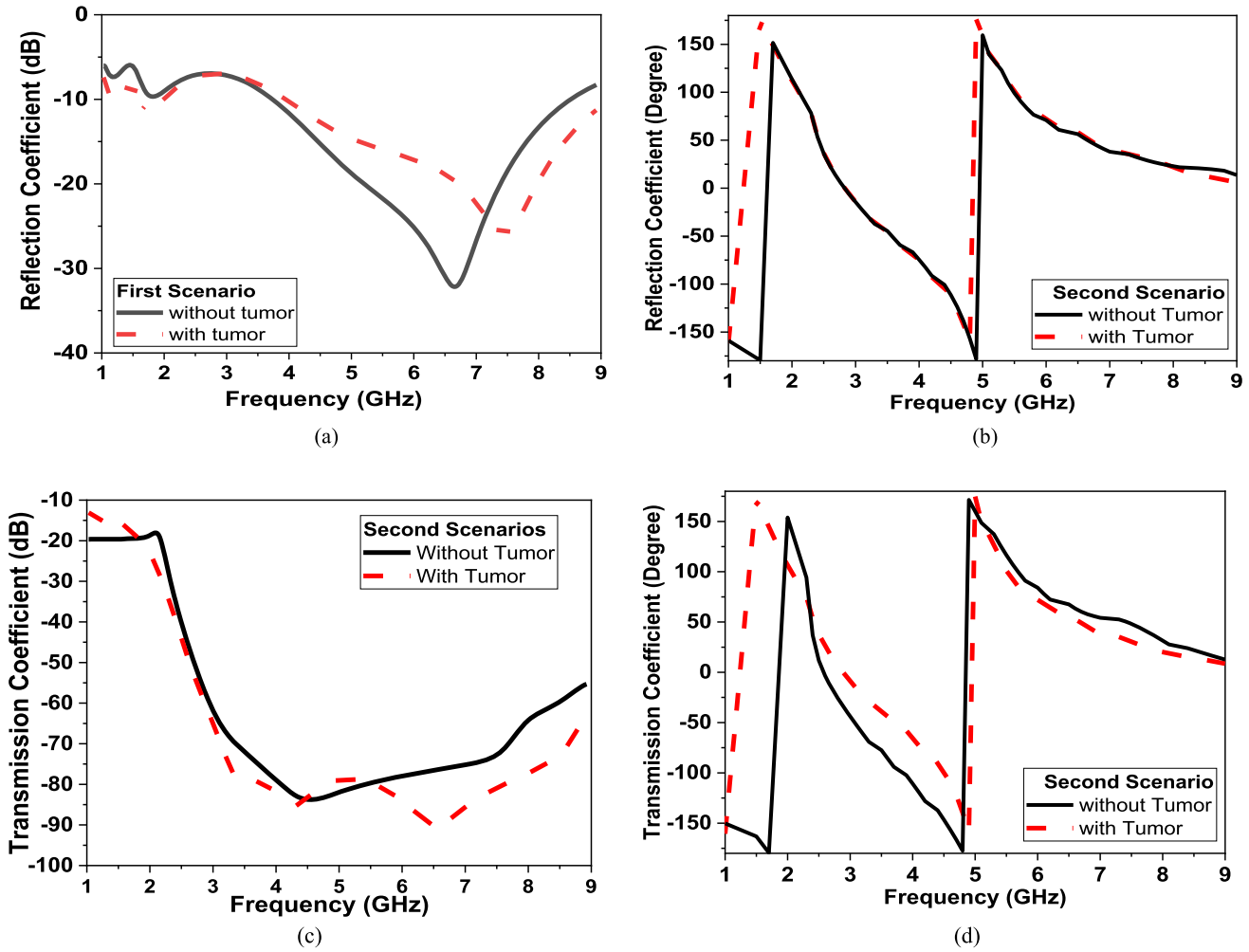

Fig. 14 Simulation of two rectangular monopole antennas with breast model **a** magnitude $|S_{11}|$ in dB, **b** $|S_{11}|$ phase in degrees **c** magnitude $|S_{21}|$ in dB and **d** $|S_{21}|$ in degrees (Color figure online)

coefficient by 10 dB and reduced the resonant by 500 MHz. For circular monopole, the tumor increased the magnitude of the reflection coefficient by 3 dB and induced a shift of 50 MHz at lower resonant band at 3.7 GHz. At higher resonant frequency at 5.5 GHz, it changes the magnitude of reflection coefficient by 2 dB and reduced the resonant by 50 MHz as shown in Fig. 13. In Fig. 14, using two rectangular antennas and embedding the tumor model induced a shift of 500 MHz in resonant frequency, reduced the reflection by 8 dB and induced around 300° phase shift. On the other side, same previous tests are done for circular monopole, the tumor induced a shift of 300 MHz in resonant frequency, reduced the reflection by 10 dB and induced around 100° phase shift. Thus, using two monopole antennas on the breast sides provides more data required to detect tumors as shown in Figs. 14 and 15. The given simulations in this paper show that it is very difficult to detect tumor with diameter less than 5 mm.

Given that the proposed sensors are designed to be embedded in women's clothes or in contact to human body, the SAR values are calculated using CST simulator, Ver. 2020. SAR or the specific absorption rate is defined as the amount of power absorbed per unit mass of tissue as reported in [19]. The simulated SAR is calculated by placing the antenna model on the phantom tissue model as shown in Fig. 16. The numerically safe SAR values at resonance frequency at 1 g and 10 g of tissue based on the IEEE C95.3 standard for a device are1.6 W/Kg and 2 W/Kg respectively. For the rectangular monopole, it realizes calculated SAR values of 2.32 W/Kg and 0.98 W/Kg as shown in Fig. 16. However, circular monopole antenna is 3.66 W/Kg and 0.98 W/Kg, respectively at 100 mW transmitted power. Safety SAR levels could be maintained for the proposed textile antennas as long as transmitted power do not exceed 100 mW. Thus, the proposed antenna could be embedded in wearable applications. From given results, the simulated SAR values of rectangular monopole antenna is less than the circular shape.

In addition, in order to study the effect of the breast density on detecting tumors as well as the dielectric properties, the

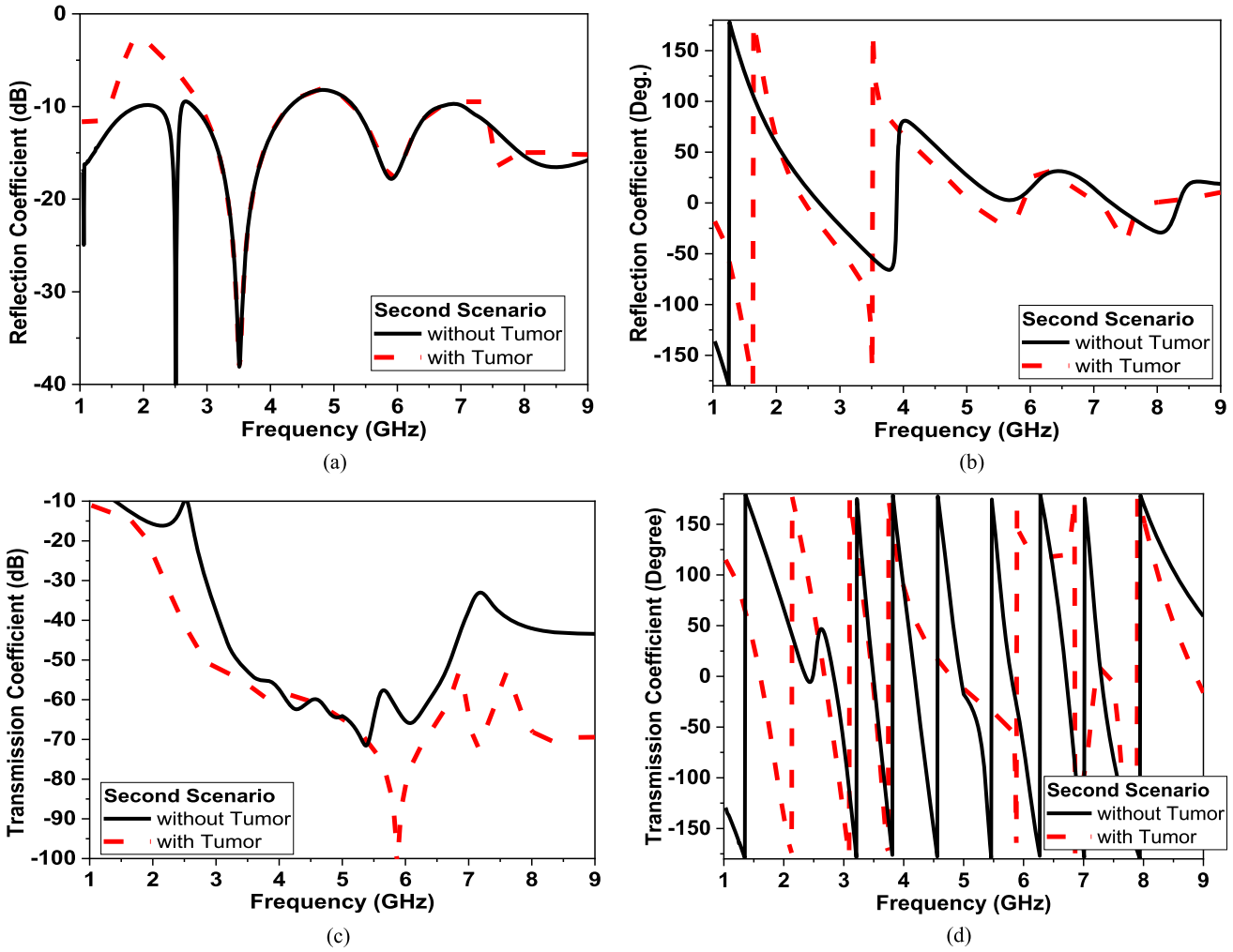

Fig. 15 Simulation of two circular monopole antennas with breast model **a** magnitude $|S_{11}|$ in dB, **b** $|S_{11}|$ phase in degrees **c** magnitude $|S_{21}|$ in dB and **d** $|S_{21}$ |in degrees (Color figure online)

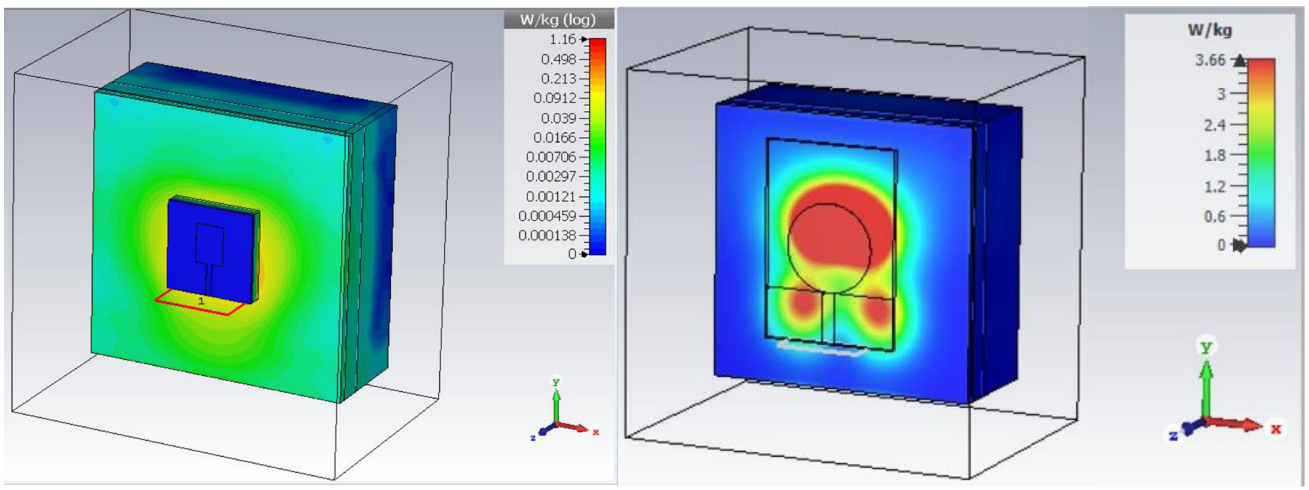

Fig. 16 SAR Simulation of textile monopole antennas with breast phantom model over 1 g of tissue based (Color figure online)

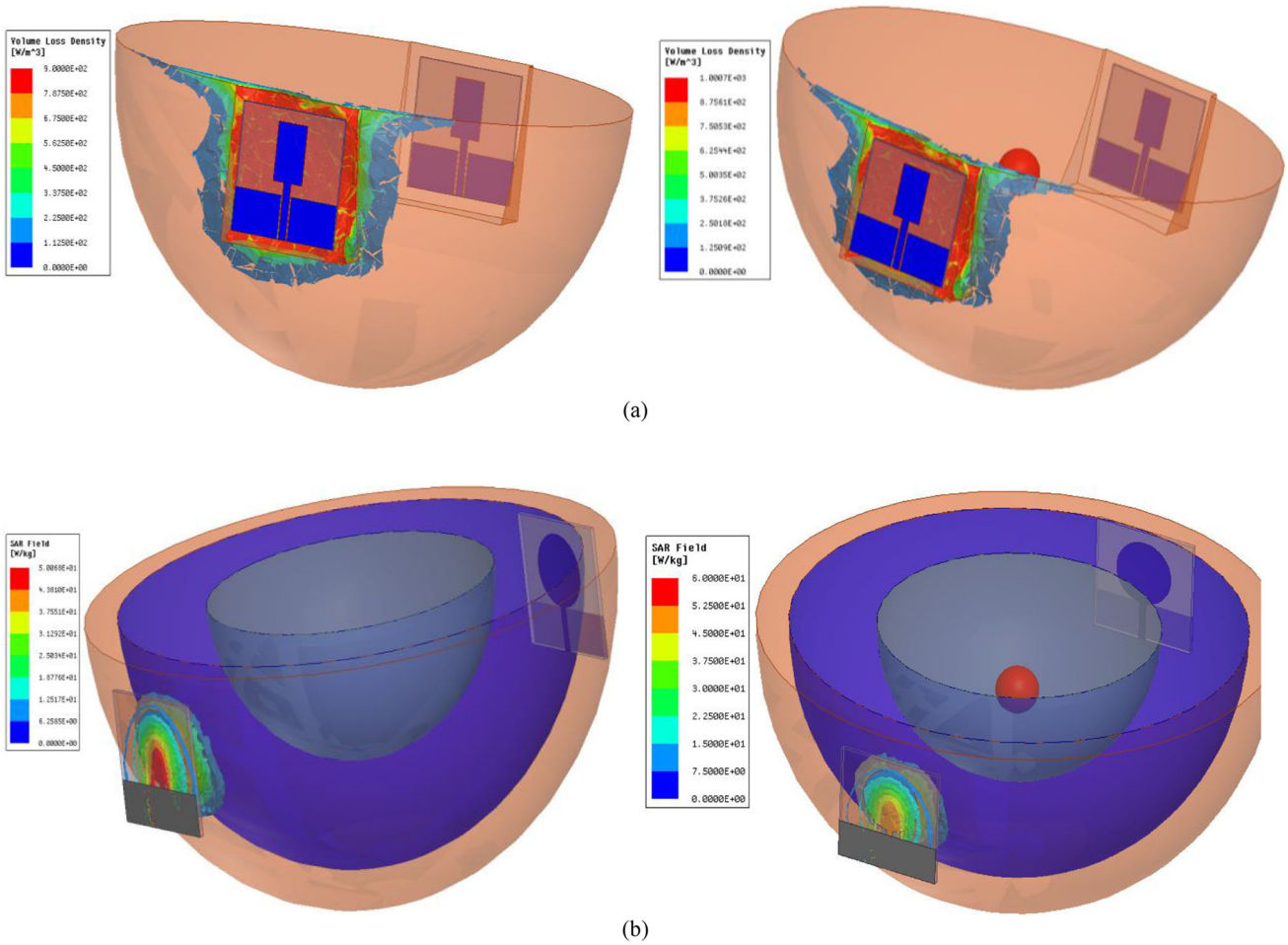

Fig. 17 **a** The volume loss density for rectangular monopole antenna without & with tumor and **b** the average SAR for circular monopole antenna without & with tumor (Color figure online)

current density and volume loss density in case of a healthy tissue and malignant tumor tissue is calculated and presented as shown in Fig. 17. The given results show that a little increase in the gain values occurred in the presence of tumor compared to the case of normal tissues as shown in Fig. 17.

5 Measured of textile antenna in proximity to breast phantom model

The proposed antennas are tested in the presence of breast phantom with and without tumour. The response of the antenna is measured while placing the phantom in glass and plastic containers. This could be related to gelatinous nature of phantom that don't tolerate high temperature nor was it mechanically durable during measurements. Gelatinous phantom representing breast is composed of 150 ml corn oil, 50 ml deionized water, 30 ml neutral detergent and 4.5 g agarose as per the recipe in [27]. On the other hand, tumor phantom is composed of 100 ml deionized tri-distilled water, 60 ml ethanol, 1 g NaCl and 1.5 g agarose [28, 29]. All prepared mixtures for breast and tumor phantoms are let to cool down and set to a gelatinous constancy. All containers carrying phantoms are sanitized to avoid any impurities and keep the electrical properties of the fabricated phantoms. The electrical properties of all phantoms (breast & tumor) are characterized using Dielectric probe **DAK-3.5-TL2:** 200–20 GHz. The measured dielectric constant (ε_r), loss tangent (ε") and conductivity for both breast and tumor phantoms are shown in Fig. 18a–d. The given measured data is highly comparative to data published in literature for electrical properties of breast and tumor [19].

The proposed antennas are tested in the presence of fabricated breast phantom with and without tumor. The measured reflection coefficient results are shown in Fig. 19 for both rectangular and circular monopoles. Figure 19 and Table 1 shows the comparison of the two proposed monopoles shaped (rectangular/ circular). In spite of this measurement method, it yields the expected desirable results. From the given results in this work and Table 1, Circular monopole

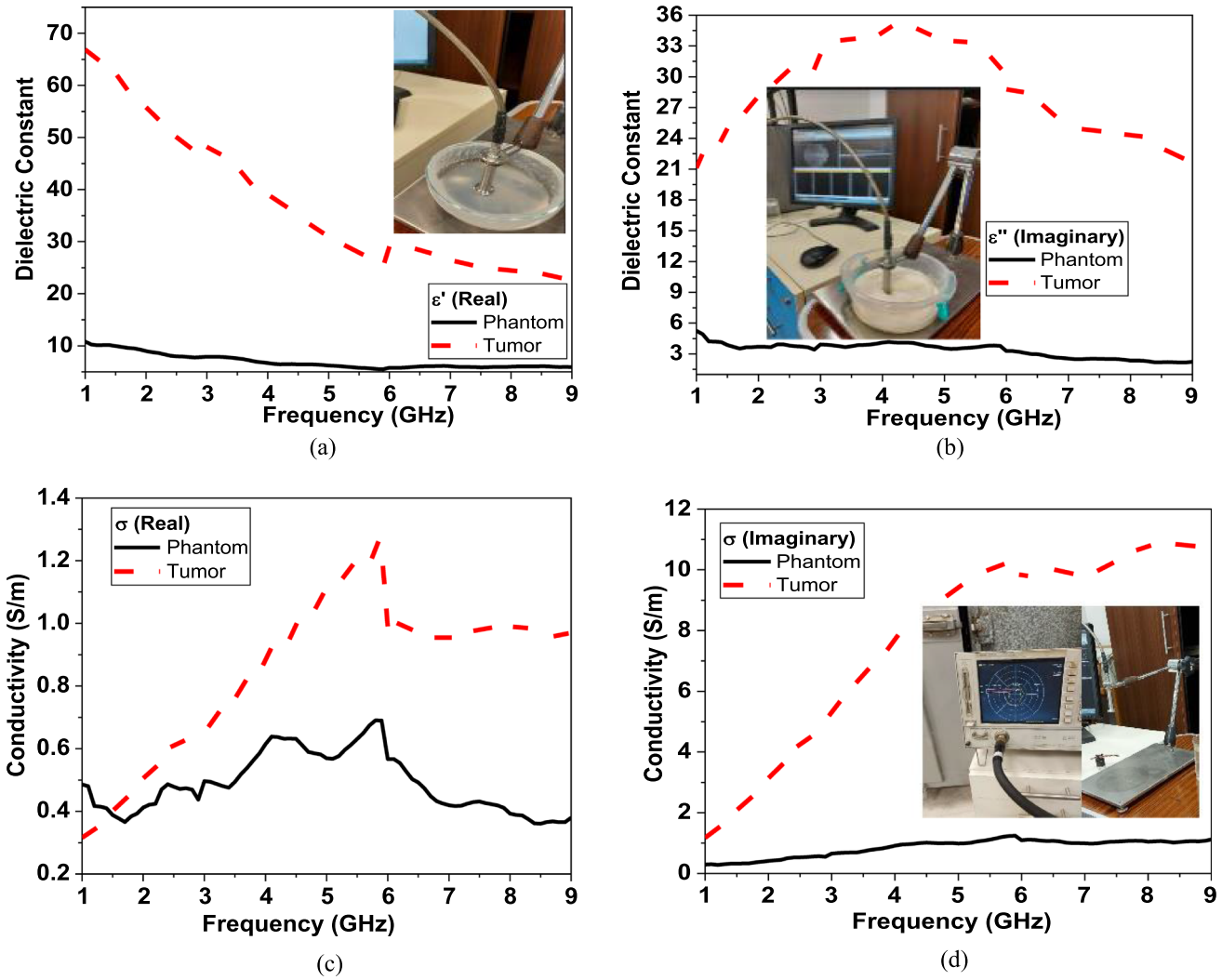

Fig.18 Breast phantom and tumor measured dielectric properties by using DAK (Color figure online)

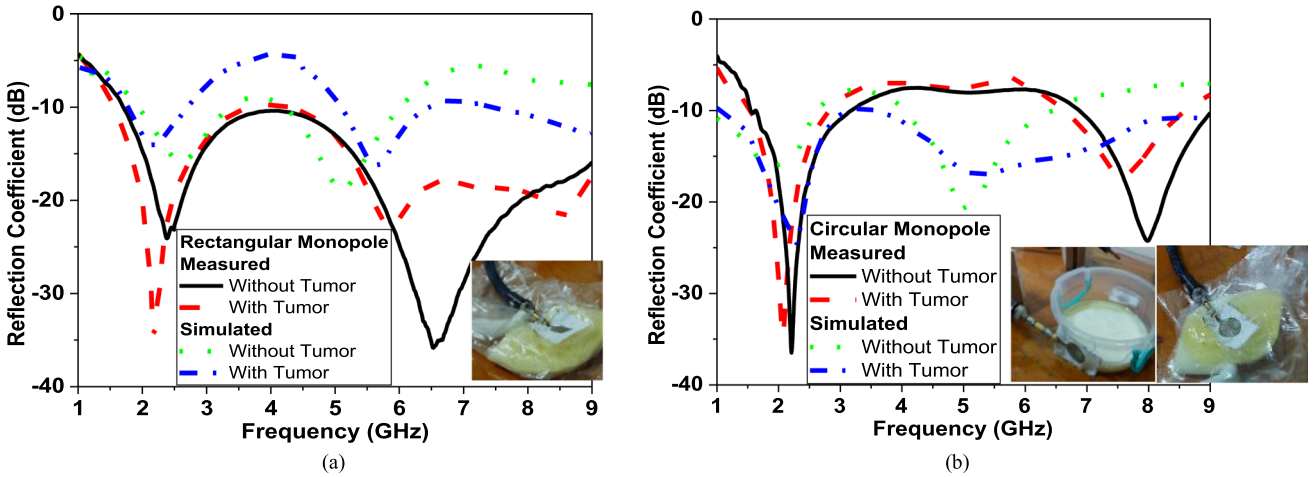

Fig. 19 Measured monopole antennas with inserted photo of breast phantom with and without tumor **a** Rectangular- shaped antenna and **b** Circular-shaped antenna (Color figure online)

Table 1 Comparison of two proposed monopoles shaped (rectangular/ circular)

Shape	Rectangular monopole	Circular monopole
Comparison		
Bandwidth	2.2 to 8 GHz	2.5 to 9 GHz
Gain	2.5 dBi	5 dBi
Power required	Low	High
Measured SAR (10 g)	0.161	0.174
Fabrication	Easy to fabricate	Hard to fabricate
Practical results	Better detection	Decent detection

acquires higher gain compared to rectangular monopole. On the other side , rectangular monopoles acquires better detection results compared to circular monopole in same band, require less power and lower SAR levels. Moreover, the proposed textile monopoles are compared to textile antennas reported in literature [29–31] and presented in Table.2. Finally, SAR values are measured in SAR Lab (Electronics Research Institute) for both proposed monopoles as shown in Table 3 at 1 g and 10 g. Table 3 shows that the rectangular-shape monopole is better in terms of SAR vales than circular shape. These results match simulation results and validate the adopted models for the proposed sensors in simulations.

6 Conclusion

This paper present two low-cost, conformal fully textile antenna-based sensor operating within the band of 2.2 to 8 GHz. The proposed monopole antennas with rectangular and circular shapes are fabricated using cotton substrate and

Table 2 Comparison of proposed antennas with similar structures in literature

Ref	Bandwidth (GHz)	Gain (dBi)	Dimensions ($W \times L \times h$) mm^3	Fabrications	SAR (W/Kg) in 10 g
[30]	2.38–2.58	NM	70 × 70 × 3	Difficult (four layers)	0.23
[17]	7–28	Peak 10	60 × 50 × 0.7	Moderate (two layers)	1 in average
[31]	8–12	Peak 5.6	37.5 × 44.33 × 1	Easy (one layer)	0.72
Proposed	2–8	Average 4	50 × 50 × 2	Easy (one layer)	0.16

NM (not mention in the paper)

Table 3 Comparison of measured SAR levels for the two proposed monopoles (rectangular/ circular)

Power level (dBm)	Rectangular monopole		Circular monopole	
	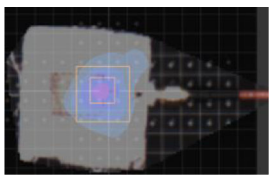 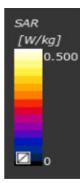		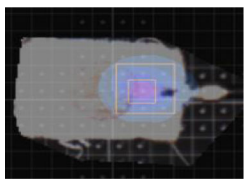 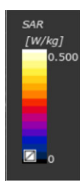	
	1 g	10 g	1 g	10 g
5	0.099	0.041	0.103	0.043
10	0.123	0.05	0.132	0.057
15	0.323	0.124	0.384	0.15
20	0.372	0.161	0.414	0.174

textile conductor with overall size 50 × 50 mm^2. The proposed textile sensor retains its operation after subjected to washing and dryness. The rectangular and circular monopole antennas are fabricated and tested. Recorded results using one and two sensors in contact with breast model verify the ability of the proposed sensor to differentiate between normal and malignant breast tissues. The proposed monopole antennas provide measured SAR value of 0.161 and 0.174 W/Kg for rectangular and circular monopoles and within safety limits with 100 mW transmitting power or less. Both proposed designs (rectangular and circular shaped) provide promising tumor detection capabilities. However, rectangular monopole shows higher sensitivity to tumor than circular monopole through recording phase shift, magnitude, and location at designed resonant frequencies. The proposed sensors are limited to detect tumors of diameter greater than 5 mm. Full parametric study representing varying tumor size and location will part of future publication. Moreover, further work to improve sensitivity of detection will be studied by using an array of sensors instead of only. Fully textile sensors are a step towards developing wearable microwave breast imaging system. This will help women to receive low-cost safe, regular breast cancer screening at the comfort of their homes.

Authors' contribution DME carried out the sensor design, simulating antenna with phantom, organizing the team work, participated in the sequence alignment, conceived of the study, and participated in its design and coordination and helped to draft the manuscript and writing the manuscript. SAA. carried out the measurements, conceived of the study, and participated in its design and coordination and helped to draft the manuscript and design the breast phantom. ARE carried out the writing the manuscript, participated in the sequence alignment and drafted the manuscript and measured the sensors. All authors read and approved the final manuscript.

Funding Open access funding provided by The Science, Technology & Innovation Funding Authority (STDF) in cooperation with The Egyptian Knowledge Bank (EKB). The authors have not disclosed any funding.

Availability of data and materials The data that support the findings of this study are openly available on the manuscript and the data underlying this article will be shared on reasonable request to the corresponding author.

Declarations

Conflict of interest We wish to confirm that there are no known conflicts of interest associated with this publication and there has been no significant financial support for this work that could have influenced its outcome. We confirm that the manuscript has been read and approved by all named authors and that there are no other persons who satisfied the criteria for authorship but are not listed. We further confirm that the order of authors listed in the manuscript has been approved by all of us. Non-financial competing interests as unpaid membership in a government or non-governmental organization, unpaid membership in an advocacy or lobbying organization and unpaid advisory position in a commercial organization.

References

1. Kaur, M., & Goyal, S. (2020). Microstrip patch antenna design for early breast cancer detection. *International Journal of Recent Technology and Engineering (IJRTE), 8*(6), 8.
2. Wang, L. (2018). Microwave sensors for breast cancer detection. *Sensors (Basel), 18*(2), 655.
3. Azubuike, S. O., Muirhead, C., Hayes, L., & McNally, R. (2018). Rising global burden of breast cancer: the case of sub-Saharan Africa (with emphasis on Nigeria) and implications for regional development: a review. *World Journal of Surgical Oncology, 16*, 1–13.
4. Ibrahim, A. S., Khaled, H. M., Mikhail, N. N., Baraka, H., & Kamel, H. (2014). Cancer incidence in Egypt: Results of the national population-based cancer registry program. *Journal of Cancer Epidemiology*. https://doi.org/10.1155/2014/437971. Epub 2014 Sep 21. PMID: 25328522; PMCID: PMC4189936.
5. Farouk, O., Ebrahim, M. A., Senbel, A., et al. (2016). Breast cancer characteristics in very young Egyptian women ≤35 years. *Breast Cancer (Dove Med Press), 8*, 53–58.
6. Kwon, S., & Lee, S. (2016). Recent advances in microwave imaging for breast cancer detection. *International Journal of Biomedical Imaging, 2016*, 5054912.
7. Loughlin, D. O., Halloran, M. O., Moloney, B. M., Glavin, M., Jones, E., & Elahi, M. A. (2018). Microwave breast imaging: Clinical advances and remaining challenges. *IEEE Transactions on Biomedical Engineering, 65*(11), 2580–2590.
8. Rahayu, Y., & Wanuwu, I. (2019). Early detection of breast cancer using ultrawideband slot antenna. *Journal by Sinergi, 23*, 115–122.
9. Porter, E., Bahrami, H., Santorelli, A., Gosselin, B., Rusch, L. A., & Popović, M. (2016). A wearable microwave antenna array for time-domain breast tumor screening. *IEEE Transactions on Medical Imaging, 35*(6), 1501–1509.
10. Srinivasan, D., & Gopalakrishnan, M. (2019). Breast cancer detection using adaptable textile antenna design. *Journal of Medical Systems, 43*(6), 177.
11. Moloney, B. M., Loughlin, D. O., Abd Elwahab, S., & Kerin, M. J. (2020). Breast cancer detection—a synopsis of conventional modalities and the potential role of microwave imaging. *Diagnostics, 10*(2), 103.
12. Borja, B., Tirado-Mendez, J. A., & Jardon-Aguilar, H. (2018). An overview of UWB antennas for microwave imaging systems for cancer detection purposes. *Progress In Electromagnetics Research, 80*, 173–198.
13. Lin, X., Chen, Y., Gong, Z., Seet, B.-C., Huang, L., & Lu, Y. (2020). Ultrawideband textile antenna for wearable microwave medical imaging applications. *IEEE Transactions on Antennas and Propagation, 68*(6), 4238–4249. https://doi.org/10.1109/TAP.2020.2970072

14. Shah, A., & Patel, P. (2021). Suspended embroidered triangular e-textile broadband antenna loaded with shorting pins. *AEU-International Journal of Electronics and Communications, 130*(153573), 1–12. https://doi.org/10.1016/j.aeue.2020.15357
15. Kirtania, S. G., Elger, A. W., Hasan, M. R., Wisniewska, A., Sekhar, K., Karacolak, T., & Sekhar, P. K. (2020). Flexible antennas: A review. *Micromachines, 11*(9), 847. https://doi.org/10.3390/mi11090847
16. Khan, M. A., Raad, R., Tubbal, F., Theoharis, P. I., Liu, S., & Foroughi, J. (2021). Bending analysis of polymer-based flexible antennas for wearable, general IoT applications: A review. *Polymers, 13*(3), 357. https://doi.org/10.3390/polym13030357
17. Mahmood, S. N., et al. (2021). Full ground ultra-wideband wearable textile antenna for breast cancer and wireless body area network applications. *Micromachines, 12*(3), 322. https://doi.org/10.3390/mi12030322
18. Atrash, M. E., Abdalla, M. A., & Elhennawy, H. M. (2021). A fully-textile wideband AMC-backed antenna for wristband WiMAX and medical applications. *International Journal of Microwave and Wireless Technologies, 13*(6), 624–633. https://doi.org/10.1017/S1759078720001397
19. D. Elsheakh and A. R. Eldamak, Microwave textile sensors for breast cancer detection, 38th National Radio Science Conference (NRSC 2021), Mansoura, May 18-20, 2021.
20. Shrestha, S., Agarwal, M., Ghane, P., & Varahramyan, K. (2012). Flexible microstrip antenna for skin contact application. *International Journal of Antennas and Propagation., 2012*, 5. Article ID 745426.
21. H. R. Khaleel, H. M. Al-Rizzo, and A. I. Abbosh, "Design, fabrication, and testing of flexible antennas," InTech, 2013, ch 15, pp. 363–383.
22. Raad, H. K., Al-Rizzo, H. M., Abbosh, A. I., & Hammoodi, A. I. (2016). A compact dual band polyimide based antenna for wearable and flexible telemedicine devices. *Progress In Electromagnetics Research C, 63*, 153–161.
23. Monne, M. A., Lan, X., & Chen, M. Y. (2018). Material selection and fabrication processes for flexible conformal antennas. *International Journal of Antennas and Propagation, 2018*, 1–14.
24. H. D. Nguyen et al., "RF characterization of flexible substrates for new conformable antenna systems," 2016 10th European Conference on Antennas and Propagation (EuCAP), 2016, pp. 1–5, https://doi.org/10.1109/EuCAP.2016.7481400.
25. Gibbins, D., Klemm, M., Craddock, I. J., Leendertz, J. A., Preece, A., & Benjamin, R. (2010). A comparison of a wide-slot and a stacked patch antenna for the purpose of breast cancer detection. *IEEE Transactions on Antennas and Propagation, 58*, 665–674.
26. Kahar, M., Ray, A., Sarkar, D., & Sarkar, P. P. (2014). A UWB microstrip monopole antenna for breast tumor detection. *Microwave and Optical Technology Letters, 57*, 49–54.
27. Romeo, S., Di Donato, L., Mario Bucci, O., Catapano, I., Crocco, L., Rosaria Scarfı, M., & Massa, R. (2011). Dielectric characterization study of liquid based materials for mimicking breast tissues. *Microwave and Optical Technology Letters, 53*(6), 1276–1280.
28. N. Joachimowicz, B. Duchêne, C. Conessa and O. Meyer, "Easy-to-produce adjustable realistic breast phantoms for microwave imaging," 2016 10th European Conference on Antennas and Propagation (EuCAP), 2016, pp. 1–4, doi: https://doi.org/10.1109/EuCAP.2016.7481715.
29. Rydholm, T., Fhager, A., Persson, M., Geimer, S. D., & Meaney, P. M. (2018). Effects of the plastic of the realistic GeePS-L2S-Breast phantom. *Diagnostics (Basel)*. https://doi.org/10.3390/diagnostics8030061
30. Yao, L., Li, E., Yan, J., Shan, Z., Ruan, X., Shen, Z., Ren, Y., & Yang, J. (2021). Miniaturization and electromagnetic reliability of wearable textile antennas. *Electronics, 10*, 994. https://doi.org/10.3390/electronics10090994
31. Jebali, N. (2020). Textile ultra-wide band antenna with X band for breast cancer detection. *Indian Journal of Science and Technology, 13*, 1232–1242. https://doi.org/10.17485/ijst/v13i11.150103_2020

Dalia M. Elsheakh (Senior Member, IEEE 2019) received the B.Sc., M.Sc., and Ph.D. degrees from Ain Shams University, in 1998, 2005, and 2010, respectively. Her M.S. Thesis was on the design of microstrip PIFA for mobile handsets and the Ph.D. Thesis was on electromagnetic band-gap structure. She was an Assistant Researcher with the HCAC, College of Engineering, University of Hawai'i, USA, in 2008, and an Assistant Professor, in 2014 and 2018. From 2010 to 2015, she was an Assistant Professor with the Microstrip Department, Electronics Research Institute, where she has been an Associate Professor, since 2016. From 2021 until now, she was a Professor with the faculty of Engineering and Technology, Badr University in Cairo. She has published 70 articles in peer-refereed journals, 45 papers in international conferences, four books chapters. She holds two patents and she is attend and chaired several national and international conferences. She is currently a member of many contracted projects (13-research and development project) as member such as ASRT, NTRA, NSF, ITDA and STDF and PI funded from funding agency, ITDA. She is a reviewer at different International Journal. She has very good experience in textile engineering for wireless communication and biomedical.

Soha A. Alsherif She was born in 1997 and graduated from high school from abroad (Saudi Arabia) and joined Ain Shams University of Engineering and graduated in 2021 and now she works at Orange Business Service as a communications engineer. The field of microwaves, optics and networks are among the fields that she was most interested in.

Angie R. Eldamak received her B.Sc. and M.Sc. degrees in electrical engineering from Ain Shams University, Cairo, Egypt, in 2002 and 2006, respectively, and Ph.D. degree in electrical engineering from Ryerson University, Toronto, Canada, in 2013. Since November 2014, she has been with the Electronics and Communications Engineering Department, Ain Shams University and she is currently an Associate Professor. She was an Assistant Researcher with Microwave Electronics Lab, University of California, Los Angeles, USA, from 2006–2007, and General Associate in Applied Electromagnetics Group at University of Calgary, CANADA from 2016–2018. She served in several units at Faculty of Engineering including Quality Assurance, E-learning, Alumni and International collaboration. From August 2021, she is appointed as International Agreements and Alumni Relations Coordinator for Faculty of Engineering and Adjunct Associate Professor at American University in Cairo. Her current research interests include electromagnetic waves, antennas, biosensors, flexible sensors fiber-based systems as well as pedagogy, courses development and accreditation for Higher Education level. She authored more than 20 peer reviewed papers in her field and serves as a peer reviewer for several international and national journals and conferences.